Research on Test Method for Vibration Characteristics of Propeller Propulsion System of Offshore Platform

Research on Test Method for Vibration Characteristics of Propeller Propulsion System of Offshore Platform

Baoping Zeng [1], Chao Xiang [1, 2, *], Yajun Gong [1]

[1] Wuhan Second Ship Design and Research Institute, Wuhan 430205, China
[2] School of Mechanical Science and Engineering, Huazhong University of Science and Technology, Wuhan, China

*Corresponding author email: xiangchao007@126.com

Abstract. The cause of abnormal noise in propeller propulsion system of a self-propelled offshore platform and its transmission path are analyzed by means of test and measurement. By collecting the vibration acceleration of propeller propulsion system components and key points based on their installation at different speeds of the driving motor, the location of the noise source and its main transmission path is realized by using the method of spectrum analysis. The method presented in this paper can be used for reference in similar vibration and noise problems.

1. Introduction

When the propeller propulsion system of a self-propelled offshore platform works, the installation base and cabin of the propulsion system appear severe abnormal vibration accompanied by large structural noise. Field staff response: the higher the speed of the motor, the more violent the abnormal vibration. In order to find the source of abnormal vibration and its transmission law, the possible vibration source and transmission path were analyzed by collecting the vibration acceleration response of the key parts of the platform propulsion system. According to the analysis results, an engineering improvement scheme for eliminating abnormal vibration is given [1-3].

2. Vibration Testing Method

A vibration system can be divided into three parts: excitation source, transmission path and response point, as shown in Figure 1.

Fig. 1 Composition of Vibration System

The excitation sources include: unbalanced mass of motor, rotating parts, unbalanced hydrodynamic force of propeller, random wave load, impact caused by friction/clearance of pairs of motion, etc., and are investigated separately.

Transfer path refers to the path from excitation source to response point to transfer energy through structural vibration. The main two transmission paths are: (1) motor-> bearing seat (between motor and

transmission shaft) ->motor drive shaft-> bearing seat (between transmission shaft and reducer) ->transmission-> transmission flange ->working cabin floor; (2) propeller ->propeller drive shaft-> transmission flange ->working cabin floor.

Response points should be located in the key positions of the two paths. Vibration source characteristics and transmission paths are preliminarily analyzed by collecting vibration acceleration responses under working conditions. Its basic principles are as follows:

Motor and motor drive system, transmission and flange, propeller and propeller drive system, working cabin floor and so on constitute a complex vibration system. When the excitation of the vibration source is transmitted to the flange and the working cabin floor through a certain path, the vibration response of the flange and the working cabin floor will occur. If the vibration source is transient (such as unit pulse), the response point will vibrate at the natural frequency of the system, that is, free vibration, and the vibration of the weakly damped system will decay rapidly. When the excitation frequency approaches the natural frequency of the system, resonance occurs, and the vibration energy increases significantly.

Therefore, the frequency characteristics of the vibration source can be analyzed by the frequency spectrum of the response point, and then the vibration source can be found. The main transmission path of the vibration energy can be preliminarily judged by the relative magnitude of the vibration acceleration of each point on the transmission path. That is to say, the strength of vibration and its main frequency components are closely related to fault types, locations and causes. By analyzing the time-domain and frequency-domain curves of the measured points of the vibration system, the approximate transmission path of the vibration can be deduced, and the approximate range of the fault can be determined. Then the main frequency components of abnormal vibration are analyzed, and the excitation force with the same frequency can be considered as the main source of vibration [4].

2.1. Test Equipment

Based on the above principles, and combined with the abnormal vibration observed in many physical prototype tests, the test scheme is formulated. The main test equipment include: 1 LMS SCADAS Mobile SCM05 data acquisition front-end, 17 unidirectional acceleration sensors, 1 three-directional acceleration sensor, 18 dedicated high fidelity data lines, a set of LMS Test. Lab 12A vibration signal acquisition and analysis software system and a laptop computer.

LMS SCADAS hardware is famous for its excellent performance and high reliability. Both laboratory and field tests can ensure the optimal test quality and accuracy. LMS SCADAS Mobile SCM05 front-end and LMS Test. Lab 12A real-time analysis software can be seamlessly integrated into a powerful sound-vibration analyzer and recorder to ensure the accuracy and compatibility of data. Fig. 2 is a data acquisition device in the field.

Fig. 2 Data acquisition device and data analysis software

In this experiment, the location of the test points is shown in Figure 3-4. The default test direction is Z, and some of the test points have marked the test direction.

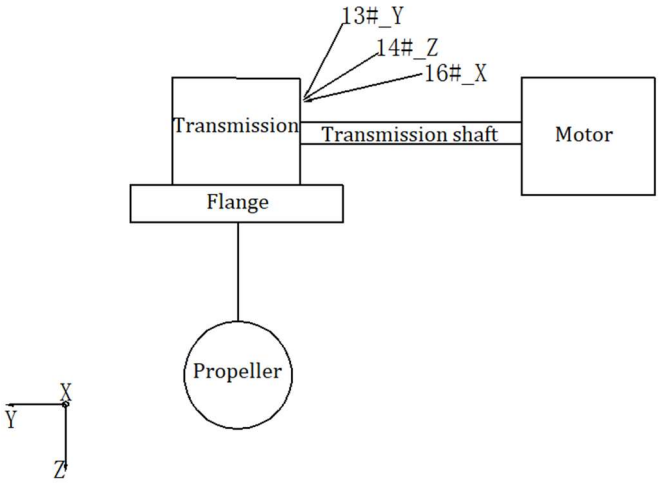

Fig. 3 Propulsion system and survey point layout

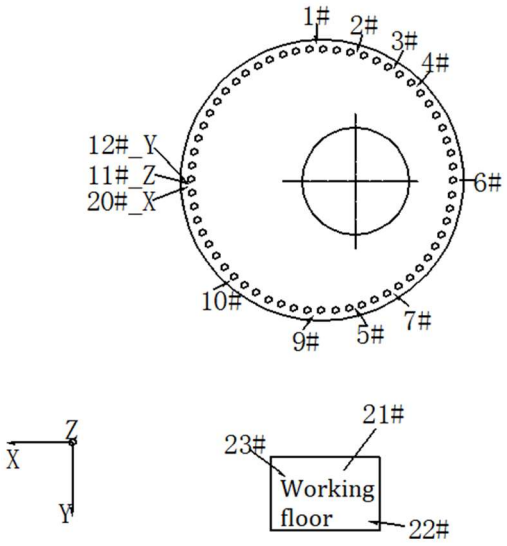

Fig. 4 Layout of measuring points

3. Test Data Processing and Analysis

3.1. Test results and analysis

The vibration signals measured in engineering are generally time domain signals, which describe the change of vibration signals with time. In the analysis of vibration signals, through the analysis of time domain waveform, we can get some relevant information, such as amplitude, period, phase, which is helpful to the analysis of vibration causes and the study of vibration mechanism. At the same time, as the most original signal of vibration analysis, time domain waveform provides the most real and comprehensive information.

However, the occurrence and development of faults often lead to the change of signal frequency structure, and these faults will appear corresponding frequency components in vibration signals. In order

to get more accurate fault information, we can transform the time domain signal of vibration into frequency domain signal by Fourier transform method, that is, signal with frequency as independent variable. The spectrum curves of acceleration response under various working conditions are listed below.

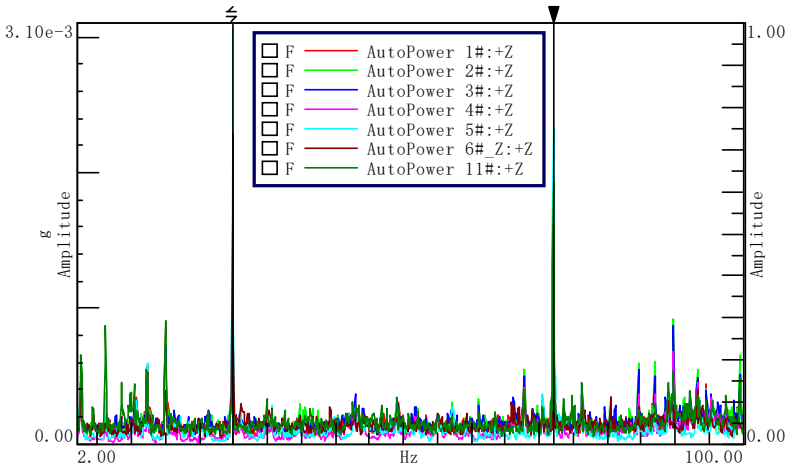

Fig. 5 Spectral curves of Z-direction acceleration response of some measuring points at the average speed of 298 r/min

Fig. 5 is the spectrum curve of acceleration response at some measuring points when the average speed of the motor is 298r/min. It can be seen from the figure that the frequency components of each line have a high similarity. The frequency points of peaks on the line are 2.48, 5.85, 10.33, 14.98, 24.91, 30.04, 49.38, 71.60, 76.19, 84.68, 89.81 (unit: Hz), etc. At this time, the fundamental frequency of motor rotation is about 5Hz, and the spectrum shows obvious order characteristics. Except that 2.48Hz is 1/2 fractional harmonic of frequency conversion, other peak frequency points can be regarded as primary or higher harmonic of frequency conversion. Among them, the fifth and fourteenth order eigenvalues of the fundamental frequency (corresponding frequency components are 24.91Hz and 71.60Hz respectively) are the most prominent, that is, the vibration energy mainly concentrates on the two order eigenvalues.

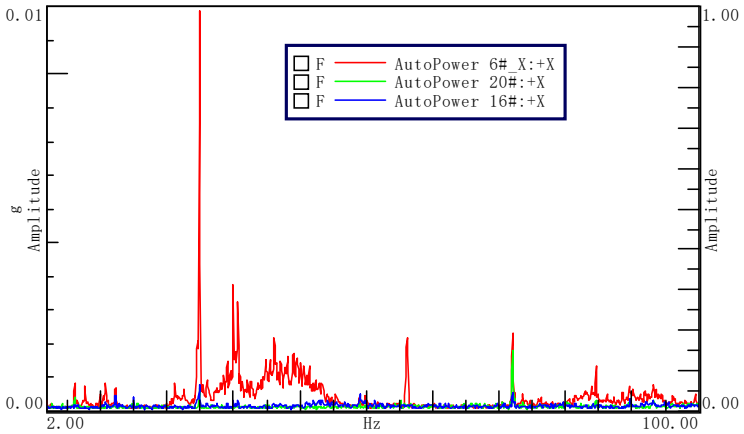

Fig. 6 Spectral curve of X-direction acceleration response of part of the measurement points

Fig. 6 is the spectrum curve of X-direction acceleration response of some measuring points when the average speed of the motor is 298r/min. From the figure, it can be seen that the vertical spectrum lines with energy concentration appear at the frequency points of 24.91 Hz, 30.04 Hz, 56.15 Hz and 71.60 Hz, especially at 24.91 Hz. These frequency points are the fifth, sixth, eleventh and fourteenth order characteristic components of frequency conversion, respectively. At the same time, it is found that the X-direction acceleration response of 6# measuring point is larger than that of other measuring points. At the frequency point of 24.91Hz, there is a vertical spectrum line of energy concentration, and the peak value is large. The resonance of 6# measurement point may occur at this frequency. At the same time, it can be found that the peak frequency point, i.e. the frequency component of the spectral line, is significantly increased compared with the X-direction of 16 # and 20 # measurement points. This may be due to the influence of seawater on the X-direction pulsating excitation force of the propeller at the 6 # measuring point at the same time (due to the eccentric placement of the propeller drive shaft, the influence of this excitation force on the 6 # measuring point is more significant).

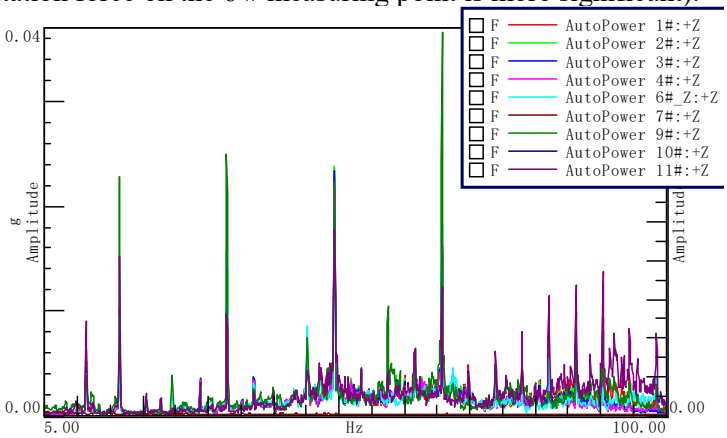

Fig.7 Spectral curve of Z-direction acceleration response of some measuring points at the average speed of 800 r/min.

Fig. 7 is the spectrum curve of Z-direction acceleration response of some measuring points when the average speed of the motor is 800 r/min. The frequency points of peaks on the spectral lines are 11.39, 16.46, 20.61, 22.61, 24.45, 28.76, 32.75, 37.06, 45.05, 49.35, 53.50, 57.49, 61.49, 65.79, 69.79, 73.94, 78.09, 82.08, 86.23, 88.54, 90.53, 92.07, 94.53, 98.52 (unit: Hz). Among them, 16.46, 32.75, 49.35, 65.79 and 98.52 (unit: Hz) show obvious order characteristics, that is, they can be regarded as the first or higher harmonics of 16.46 Hz.

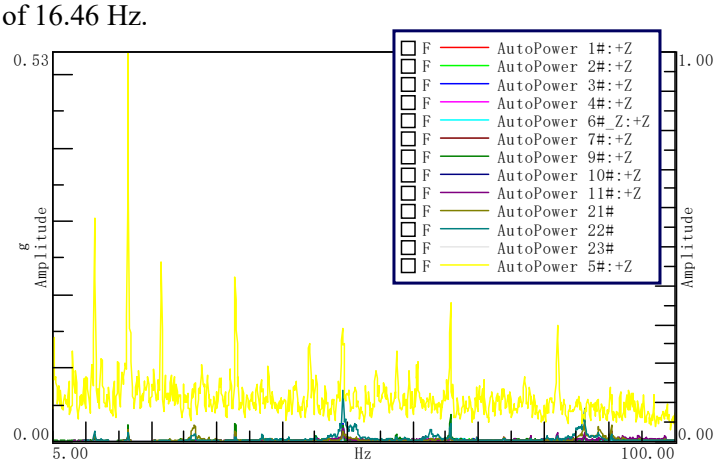

Fig.8 Spectral curves of Z-direction acceleration response at all measuring points

Fig. 8 is the spectrum curve of Z-direction acceleration response of all measuring points when the average speed of the motor is 800 r/min. It can be seen from the graph that the spectrum curve of Z-direction acceleration response of 5# measuring point under this working condition shows similar characteristics to that of working condition 4 and 6. The specific reasons have been explained before, and will not be repeated here.

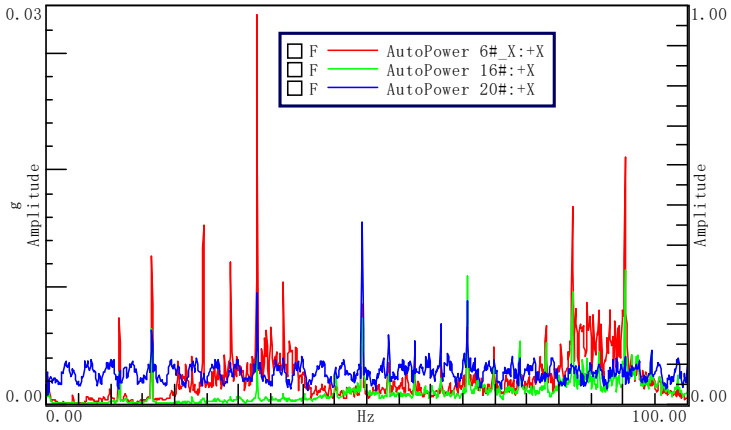

Fig.9 Spectral curves of the X-direction acceleration response of the measured points

Fig. 9 is the spectrum curve of X-direction acceleration response of some measuring points when the average speed of the motor is 800 r/min. It can be seen from the graph that the X-direction acceleration spectrum of the 6# measuring point is still relatively high, and shows a certain order characteristics.

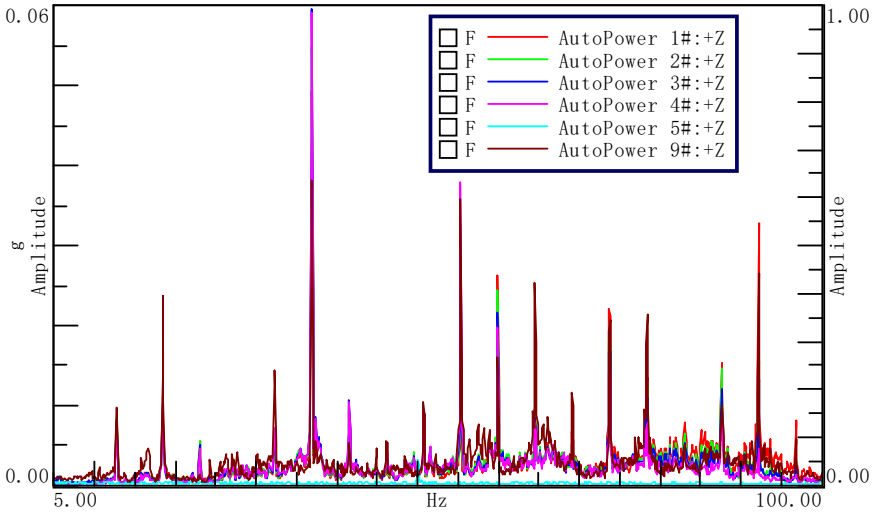

Fig. 10 Spectral curve of Z-direction acceleration response of part of measuring points at motor average speed 897r/min

Fig. 10 is the spectrum curve of Z-direction acceleration response of some measuring points when the average speed of motor is 897r/min. As can be seen from the graph, the peak frequency points on the spectrum are 12.62, 18.46, 23.07, 32.92, 36.59, 41.51, 46.12, 50.73, 55.04, 59.95, 64.56, 69.17, 73.38, 78.39, 83.16, 87.61, 91.92 (unit: Hz), etc. Among them, 18.46, 36.59, 55.04, 73.38 and 91.92

(unit: Hz) show certain order characteristics, that is, they can be regarded as the first or higher harmonics of 18.46 Hz. Of all the frequency points, 36.59 Hz is the most prominent frequency component.

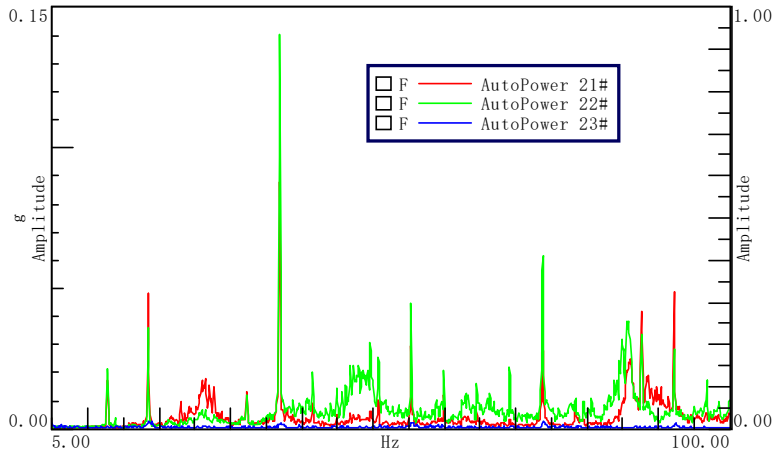

Fig. 11 Spectral curve of Z-direction acceleration response of measured points on the floor

Fig. 11 is the spectrum curve of Z-direction acceleration response of three measuring points on the floor when the average speed of the motor is 897r/min. It can be seen from the figure that the coupling resonance occurs at the frequency of 36.59 Hz at 22# measuring point. According to the RMS acceleration and maximum acceleration of each measuring point, the floor vibration also has a high contribution to the overall vibration response of the system under this condition, which can not be ignored. This further shows that floor resonance is an important source of vibration and noise in platform dynamic system.

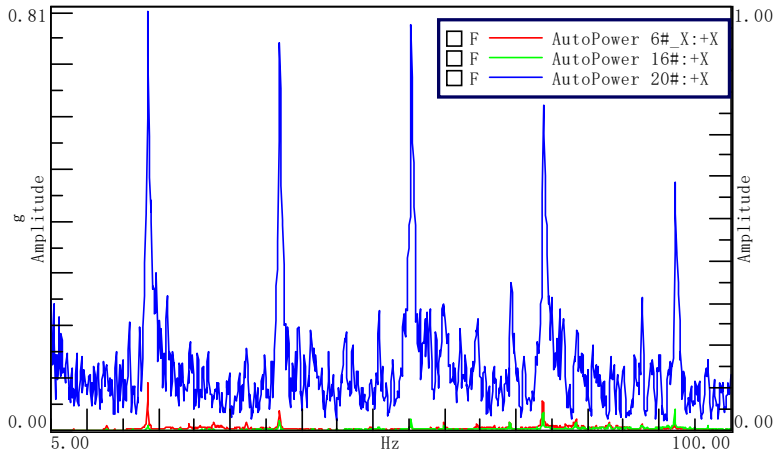

Fig. 12 Spectral Curves of X-direction Acceleration Response of Some Measuring Points at the Average Speed of Motors 897r/min

Figure 12 shows the spectrum curve of X-direction acceleration response of some measuring points when the average speed of the motor is 897r/min. From the graph, it can be seen that the three curves have vertical spectral lines of energy concentration at 18.46 Hz, 36.59 Hz, 55.04 Hz, 73.38 Hz and 91.92 Hz, showing obvious order characteristics. That is, these frequency points can be regarded as

eigenvalues of order 1, 2, 3, 4 and 5 of 18.46 Hz, respectively, which coincide with the frequency components of acceleration spectrum in Z direction of some measuring points. Among them, the X-direction acceleration value of 20 # measurement point is obviously higher, and shows a vertical spectrum with a large peak value at several order points. At this time, the amplitude of vibration acceleration at 20 # measuring point is much larger than that at other measuring points. It is worth noting that in the previous working conditions, when the average speed of the motor is below 897r/min, the X-direction acceleration spectrum of the three measuring points always shows the characteristics of 6 # measuring points whose amplitude is larger than other 20 # and 16 #, which is quite different from the phenomena under this working condition. The reasons for this phenomenon may be as follows: due to the eccentric placement of propeller drive shaft, the quality of flange on the side of 6 # measuring point is less than that on the side of 20 # measuring point. The material properties and installation status of the flange on the side of 6# measuring point are consistent with those on the side of 20# measuring point. That is, the stiffness is the same, which results in the natural frequency of the flange on the side of 6# measuring point is less than that of the flange on the side of 20# measuring point. When no resonance occurs between 6 # and 20 # measurement points, the response of 6 # measurement point is naturally greater than that of 20 # measurement point because the excitation source is closer to 6 # measurement point and the excitation force is greater. With the continuous improvement of motor speed, the frequency of excitation source is also increasing. The excitation frequency first reaches a natural frequency of 6 # measurement point, and resonance occurs at 6 # measurement point. At this time, the response of 6 # measurement point is also greater than that of 20. When the frequency of excitation source is the same as the natural frequency of a certain order at 20 # measuring point, the resonance occurs at 20 # measuring point. At this time, 6 # measuring point becomes forced vibration without resonance. The acceleration amplitude of 20 # measuring point will be larger than that of 6 # measuring point, showing the same characteristics as this working condition. That means the natural frequency of the measuring point 6# is less than the excitation frequency when the motor average speed is 897r/min. Combining with working condition 9, it can be seen that the natural frequency at 6# measuring point is 34.75 Hz. Which is less than the second harmonic of 36.59 Hz under the working condition of 18.46 Hz excitation frequency. At this time, 6# measuring point is forced vibration without resonance. Under this condition, the main source of vibration and noise is the pulsating excitation of seawater to propeller, which causes resonance at 20 # measuring point. At this time, the main vibration transmission path is: propeller-> propeller drive shaft ->transmission flange-> working cabin floor.

3.2. Reliability Test of Spectrum Analysis

Fig. 13-15 are the change curves of the RMS value of acceleration with motor speed at some key measuring points. With the increase of motor speed, the vibration energy transmitted by vibration source is also increasing. Then the RMS curve of acceleration should be an upward trend with rotational speed. If the acceleration curve shows a significant downward trend, it means that the measured point produces resonance at a certain speed of the motor, resulting in a significant increase in energy. With the increase of the motor speed, the frequency ratio of forced vibration increases, the resonance frequency far away from the measured point disappears, and the vibration energy of the measured point decreases, resulting in a downward trend of the curve. However, it should be noted that if the curve does not show a downward trend, it does not mean that there is no resonance in the working process of the propulsion system. It is also possible that resonance occurs at the same side point under two different rotational speeds, and the curve may not show a downward trend. This method can be used to test the reliability of the above spectrum analysis.

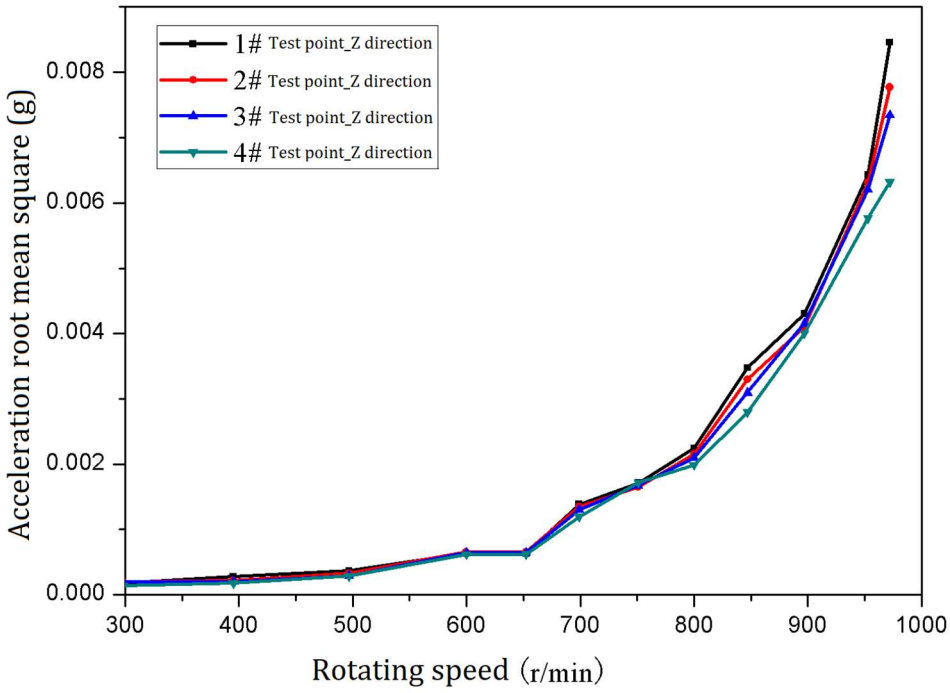

Fig. 13 Variation Curves of RMS of Acceleration at Measuring Points 1-4#

Fig. 13 shows the change curve of RMS of acceleration with rotational speed at 1-4 # measuring points. From the graph, it can be seen that the RMS value of Z-direction acceleration at 1-4 # measuring points increases with the increase of motor speed. In this process, it can not be determined whether resonance occurs or not.

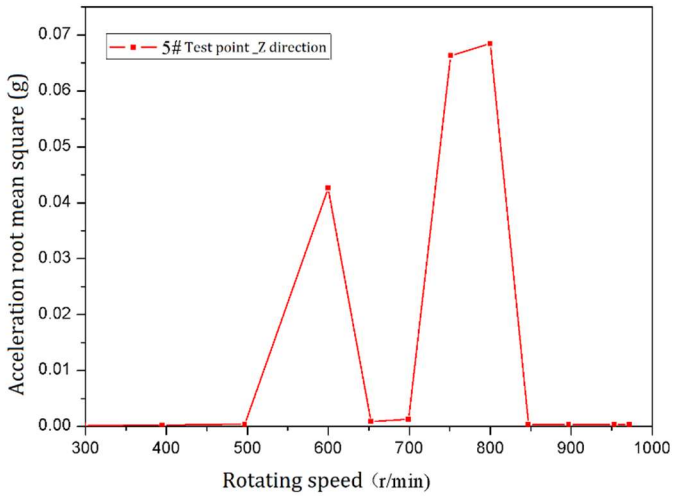

Fig. 14 Variation Curve of RMS of Acceleration at Measuring Point 5 #

Fig. 14 shows the change curve of RMS of acceleration with rotational speed at 5 # measuring point. The graph shows that the RMS value of Z-direction acceleration at 5# measuring point shows a downward trend in the range 599.7-652.5r/min and 800- 847 r/min at the average motor speed. Based on the analysis of the average motor speed under working condition 4 at 599.7 r/min and under working

condition 8 at 800 r/min, a new friction vibration source is introduced due to the resonance of bolts or flanges, thus the total energy increases. Therefore, it is normal for the 5 # test point to show a downward trend in these two intervals.

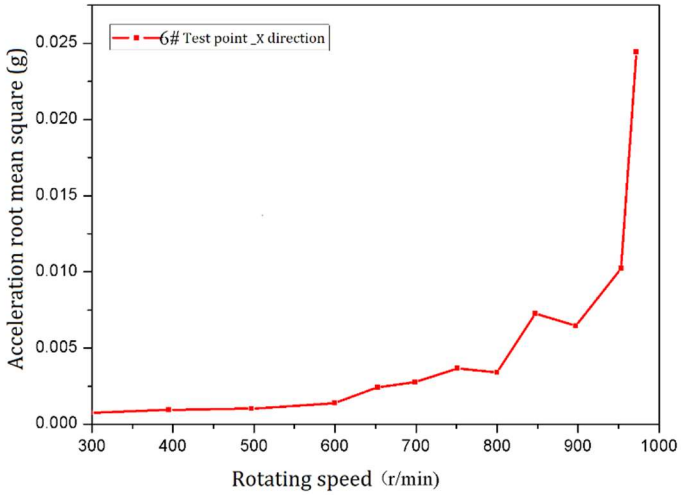

Fig. 15 Variation Curve of RMS of Acceleration at Measuring Point 6#

Fig. 15 shows the change curve of RMS of acceleration with rotational speed at 6 # measuring point. It can be seen that there is a slight decrease in the X direction of measuring point6# in the range of 751-800 r/min for the average speed of the motor, but it can not be judged that the X direction of measuring point6# has resonance in the condition of 751 r/min of the average speed of the motor. Combining with the analysis of working condition 7 and 8, it is found that the X direction of 6 # measuring point shows similar characteristics under these two working conditions, that is, the resonance may occur at the same time in working condition 7 and 8 of at the measuring point 6#. Or it may be caused by excessive excitation force of forced vibration under these two working conditions (for example, unbalanced hydrodynamic force of propeller). The small decrease of the RMS of acceleration at the measuring point 6# can not eliminate the influence of the change of excitation components and the noise interference introduced in the testing process. Coupled resonance does occur at 34.75 Hz at the measuring point 6#, and the downward trend is reasonable.

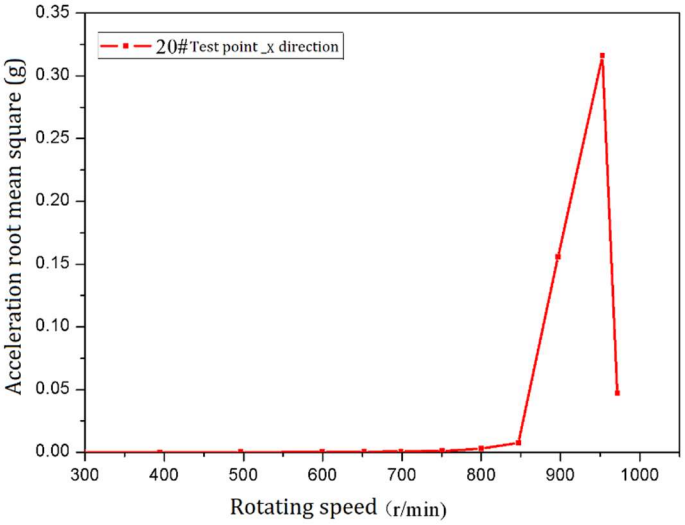

Fig. 16 Variation Curve of the RMS of acceleration at the measuring point # 20

Fig. 16 shows the change curve of the RMS acceleration in X direction at the measuring point 20# with the rotation speed. It can be seen the RMS of the X direction acceleration at the measuring point 20# shows an obvious downward trend in the range of 953 r/min to 972r/min for the average speed of the motor. Based on the analysis of working conditions 11 and 12, it can be concluded that the measuring point 20# resonates at the average motor speed of 953 r/min. With the increase of the motor speed, the excitation frequency avoids the resonance region of the measuring point 20#, and the amplitude of the average motor speed of 972r/min decreases significantly.

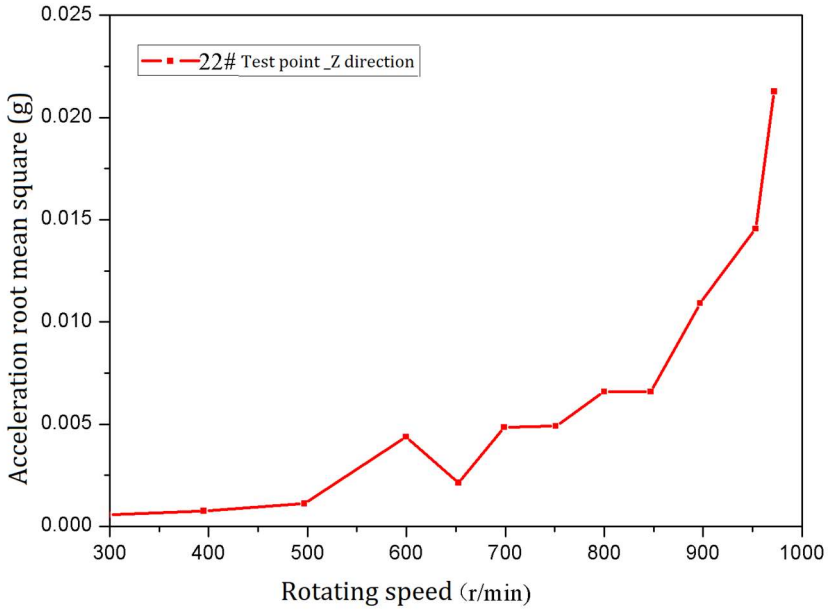

Fig. 17 Variation curve of RMS of acceleration at measuring point # 22

Fig. 17 shows the change curve of the RMS of acceleration in the Z direction of 22# measuring point with the rotation speed. As can be seen from the figure, the Z direction acceleration RMS of 22# measuring point shows an obvious downward trend in the range of 599.7 ~ 652.5r/min for the average speed of the motor. According to the analysis of working condition 4 and working condition 5, coupling resonance may occur at the measuring point of # 22 at 49.74hz at working condition 4.

4. Conclusion

After the above tests and the analysis of the test data, the following conclusions can be drawn:

(1) In the working state of the propulsion system, the excitation from the propeller is the main source of abnormal vibration. When the motor speed is high, because of the larger exciting force of the vibration source and the frequency range corresponding to the working speed of part of the natural frequency of the system, the larger vibration and noise response may be an important reason for the vibration and noise.

(2) The main transmission path of abnormal vibration is "propeller->propeller drive shaft-> transmission flange-> working cabin floor". The transmission path from the motor is not the main path.

(3) It is found that the main peak frequency of vibration is less than 100 Hz under test conditions. Because the cabin structure is complex and space thin-walled structure, according to experience, it is not excluded that the structural mode has a frequency below 100Hz. When the corresponding order frequency of a specific speed contains this modal frequency, the system has the risk of resonance, showing abnormal deterioration of the level of vibration and noise.

References

[1] Jorge Maestre, Jordi Pallares, Ildefonso Cuesta, Michael A. Scott. A 3D isogeometric BE–FE analysis with dynamic remeshing for the simulation of a deformable particle in shear flows. Computer Methods in Applied Mechanics and Engineering, 2017, Vol. 326, pp: 70-101.

[2] Sanbao Hu. Research on Multidisciplinary Topology Optimization Methods. Huazhong University of Science and Technology, Doctoral thesis, 2011

[3] Xing-an Hao, Kai Chen. Improvement of the swing platforms hydraulic system for the sizing mill. Chinese Hydraulics & Pneumatics, 2011, No. 3, pp: 69-71

[4] Michael Yu Wang, Xiaoming Wang, Dongming Guo. A level set method for structural topology optimization. Computer Methods in Applied Mechanics and Engineering, 2003, Vol 192, No. 1-2, pp: 227-246.